TRANSLATIONAL PROTEOMICS 2 (2014) 14–24

ScienceDirect

journal homepage: http://www.elsevier.com/locate/trprot

# Analysis of plasma from prostate cancer patients links decreased carnosine dipeptidase 1 levels to lymph node metastasis

*Ulrika Qundos*[a], *Henrik Johannesson*[b], *Claudia Fredolini*[a], *Gillian O'Hurley*[c], *Rui Branca*[d], *Mathias Uhlén*[a], *Fredrik Wiklund*[e], *Anders Bjartell*[f], *Peter Nilsson*[a], *Jochen M. Schwenk*[a,*]

[a] *Science for Life Laboratory, School of Biotechnology, KTH Royal Institute of Technology, Box 1031, SE-171 21 Solna, Sweden*
[b] *Atlas Antibodies AB, AlbaNova University Center, SE-106 91 Stockholm, Sweden*
[c] *Department of Immunology, Genetics and Pathology, Uppsala University, SE-751 85 Uppsala, Sweden*
[d] *Science for Life Laboratory, Clinical Proteomics Mass Spectrometry, Department of Oncology-Pathology, Karolinska Institute, Box 1031, SE-171 21 Solna, Sweden*
[e] *Department of Medical Epidemiology and Biostatistics, Karolinska Institute, Nobels väg 12 A, SE-171 77 Stockholm, Sweden*
[f] *Department of Clinical Sciences, Division of Urological Cancers, Skåne University Hospital Malmö, Lund University, SE-205 02 Malmö, Sweden*

ARTICLE INFO

*Article history:*
Received 6 August 2013
Received in revised form
2 December 2013
Accepted 2 December 2013

*Keywords:*
Sandwich immunoassay
Prostate cancer
Plasma biomarker
Suspension bead array
Carnosine dipeptidase 1

ABSTRACT

There is a need for a better differentiation of aggressive tumors in prostate cancer to design a tailored treatment for each patient, preferably by a minimally invasive analysis of blood samples. In a previous study, we discovered a decrease of plasma levels of carnosine dipeptidase 1 (CNDP1) in association with aggressive prostate cancer. Now this relation has been investigated and characterized further by generating several new antibodies for extended analysis of CNDP1 in plasma. Multi-antibody sandwich assays were developed and applied to 1214 samples from two Swedish cohorts that confirmed decreased levels of CNDP1 in plasma from patients with advanced disease. Therein, data from CNDP1 assays allowed a better differentiation between tumor N stages than clinical tPSA, but did not when classifying T or M stages. Further investigations can now elucidate mechanisms behind decreasing levels of CNDP1 in plasma and primary in regards to lymph node metastasis.



*Abbreviations:* CAB, commercial antibody; CNDP1, carnosine dipeptidase 1; CV, coefficient of variance; FDR, false discovery rate; HPA, Human Protein Atlas; GLM, general linear model; LOESS, local regression; MAB, monoclonal antibody; MFI, median fluorescence intensity; nMFi, normalized median fluorescence intensity; KW, Kruskal–Wallis one-way analysis of variance; PCa, prostate cancer.

* *Corresponding author*. Tel.: +46 852481482; fax: +46 852481425.
E-mail address: jochen.schwenk@scilifelab.se (J.M. Schwenk).

2212-9634 
http://dx.doi.org/10.1016/j.trprot.2013.12.001

## 1. Introduction

In contemporary practice, most patients with prostate cancer (PCa) are diagnosed following a PSA test and are asymptomatic at the time of diagnosis. Although serum PSA has a low specificity for prostate cancer, it can be used to single out patients with advanced disease. Efforts to improve our understanding of disease onset, diagnosis and progression through the analysis of prostate tissue, serum, plasma, urine or seminal fluid offers various entry points for discovery driven analysis. One of these is proteomics that aims at the determination of protein constituents and their isoforms in a give sample [1]. For this type of analysis several technologies are available to allow high-throughput analysis of prostate cancer samples. This includes affinity-based proteomics with a growing number of available binding molecules toward human proteins [2], and combined with microarray assays, multi-parallel immunoassays of many samples can be achieved [3].

In a previous study, we used antibodies from the Human Protein Atlas [4] and suspension bead arrays [5] to protein profile plasma from patients with prostate cancer and respective controls. There we identified the protein carnosine dipeptidase 1 (CNDP1), as a potential marker for aggressive prostate cancer. CNDP1 is a secreted protein of 57 kDa found in human blood and the central nervous system, with an approximate serum concentration of 20 μg/ml in healthy individuals [6,7] and acts as homodimer [8] and displays carboxypeptidase and dipeptidase activity, degrading carnosine and homocarnosine [9]. It is furthermore a glycoprotein that carries N-glycosylation on C-terminal residues 322 and 382 [10] and CNDP1 has been reported to form a complex with protease inhibitor alpha-2 macroglobulin [11]. Thus far, CNDP1 has been mainly mentioned with the susceptibiliy to nephropathy in type 2 diabetes through common genetic variants [12] and carnosine, substrate of the CNDP1, is believed to act as a protective factor in diabetic nephropathy [13]. A first link between CNDP1 and prostate cancer was discovered in our antibody array based analysis that revealed a decreased level of CNDP1 in plasma of patients suffering from an aggressive form of the disease [5].

The aims of this study were to improve the CNDP1 detection in plasma samples by developing multiple sandwich immunoassays and thereby to investigate the association of the decrease in CNDP1 levels with these assays in additional prostate cancer plasma samples. Further, we aimed to analyze whether the reported/predicted glycosylation status [10] or any interacting partner of CNDP1 are causing a differential detection in relation prostate cancer severity.

## 2. Materials and methods

### 2.1. Samples

Four sets of plasma samples were studied from three independent collections (see Supplementary Table 2A for details). These samples were analyzed in independent experiments and this is described in four phases (phases I–IV). This included two collections 79 heparin plasma samples (Skåne University Hospital, Sweden, denoted phase I) and 90 EDTA plasma samples (Cancer Prostate in Sweden, phase II) that had been analyzed previously using a single antibody based approach [5]. Phase III was built on 317 additional samples from CAPS. For phase IV, 728 heparin plasma samples were obtained during a collection period of 2004–2010 at Skåne University Hospital.

### 2.2. Deglycosylation and Western Blot

Plasma samples were diluted 10× in 50 mM $NaPO_4$, 0.1% (v/v) SDS and 1% Triton X100 and incubated at 96 °C for 3 min and 10U PNGaseF (Peptide-N-glycosidase F, Roche Diagnostics) were added for 24 h incubation at 37 °C. Moreover, 300 ng of recombinant CNDP1 (TP310312, Origene) were diluted and prepared as above. The extent of deglycosylation of CNDP1 was then evaluated with Western Blot with HPA-1 as detection antibody. Per lane, 50 ng of recombinant CNDP1 and 2 μg plasma samples depleted from human serum albumin (HSA) and immunoglobulin G (IgG) by the use of Affibody molecules (Affibody AB) coupled to Sulfolink matrix (Pierce) as described elsewhere [10], were loaded to an SDS-PAGE (4–12% Bis Tris, Invitrogen). Proteins were transferred onto membrane (0.45 μm PVDF, Invitrogen) according to the manufacturers protocol and transfer was confirmed with Ponceau (Pierce) staining. Membranes were blocked in 5% milk powder (Semper) in TBS-T for 1 h. Primary antibodies were incubated at optimized concentrations in blocking buffer at 4 °C for 16 h. Membranes were washed in TBS-T for 3 × 5 min followed by incubation with HRP-conjugated polyclonal swine anti-rabbit antibody (Dako) in blocking buffer at RT for 1 h. A final wash was followed by detection with TMBM substrate (Moss Inc.). The antibodies were also directly compared using a multi-screen apparatus (Mini-PROTEAN II, Bio-Rad).

### 2.3. Antibodies and epitope mapping

For the described immunoassays, different capture antibodies were utilized (Table 1 and supplementary Table 1). Monoclonal antibodies were generated in mice toward antigens 1 and 2 (Fig. 3A) and obtained from Atlas Antibodies AB, Sweden. The polyclonal detection antibody AF2489 (RnD Systems) was labeled with biotin (NHS-PEG4Biotin, Pierce) at a 50-fold molar excess over 2 h at 4 °C and stored after adding Tris-HCl (pH 8.0) at a 250-fold molar excess. All anti-CNDP1 antibodies were epitope mapped on bead arrays using 15-mer peptides with a 10 residue overlap spanning CNDP1 antigens 1 and 2 (Fig. 3A) as described previously [14]. For Alfa-2 macroglobulin, antibodies and protein standard were used from a kit (DY1913, RnD Systems).

### 2.4. Bead based sandwich assays

Antibodies were coupled to magnetic carboxylated beads (MagPlex, Luminex Corp.) according to the manufacturers protocol and as described previously [5]. The coupling efficiency for each antibody was determined via R-phycoerythrin-labeled anti-rabbit (Jackson ImmunoResearch Laboratories), Alexa Flour 555-labeled anti-goat (Invitrogen) and R-phycoerythrin-labeled anti-mouse (Moss Inc.) IgG

**Table 1 – List of antibodies directed toward (A) CNDP1 and (B) other proteins. For numeric epitope/immunogen specification, the amino acid region of the respective full-length protein is listed.**

(A) CNDP1 antibodies

| Name | Antibody ID | CNDP1 region | Epitopes | Species |
|---|---|---|---|---|
| HPA-1[a] | HPA008933 | 32–133 | 32–46; 57–76; 102–116; 122–133 | Rabbit |
| HPA-1.F1[a] | N/A | 32–133 | 32–46 | Rabbit |
| HPA-1.F15[a] | N/A | 32–133 | 102–116 | Rabbit |
| CAB-1[a,b] | AF2489 | 28–507 | 62–81; 77–96; 107–121; 387–401; 457–471 | Goat |
| MAB-1.1[a] | 3A6 | 32–133 | 47–61 | Mouse |
| MAB-1.2[a] | 5B2 | 32–133 | 47–61 | Mouse |

(B) Other antibodies

| Name | Antibody ID | Target protein | Immunogen | Homology to CNDP1 (%) |
|---|---|---|---|---|
| HPA-3[a] | HPA036899 | CNDP2 | 154–249 | 55 |
| HPA-4[a] | HPA036898 | CNDP2 | 23–96 | 53 |
| HPA-5[a] | HPA002265 | A2M | 603–748 | 7 |
| CAB-4[a] | A0001 | HSA | Full-length | 13 |
| CAB-5[a] | Rabbit IgG sera | N/A | N/A | N/A |

[a] Capture antibody.
[b] Detection antibody.

antibodies. Bead arrays were then created by combing equal amounts of beads, where each population of a distinct color-code and carrying a particular antibody. Plasma samples were thawed at RT, centrifuged for 10 min at 3000 rpm, and transferred into a microtiter plate (Abgene) according to a designed layout. The plates were centrifuged (1 min at 3000 rpm) and samples were diluted 1:10 in 1× PBS in 96-well microtiter plates with a liquid handler (TECAN, Freedom Evo 150). Samples were diluted 50× in assay buffer composed of 0.5% (w/v) polyvinyl alcohol and 0.8% (w/v) polyvinylpyrrolidone in 0.1% casein (all Sigma) in PBS supplemented with 0.5 mg/ml rabbit IgG (Bethyl Laboratories). The samples were treated in a thermocycler at 56 °C for 30 min and 23 °C for 15 min. Then, 45 μl was combined with 5 μl of a bead array in 384-well flat-bottomed half-area microtiter plates (Greiner), and incubation took place O/N on a shaker at RT and 650 rpm. Beads were washed on a magnet 3× with 100 μl of PBST (1× PBS, pH 7.4, 0.1% Tween20) using a plate washer (EL406, BioTek). This was followed by 1 h with 50 μl of 0.1 μg/ml labeled detection antibody CAB-1 (RnD Systems), 3× washing, 10 min with a solution containing 0.1% paraformaldehyde in PBS. Beads were washed again, and 50 μl of 0.5 μg/ml R-phycoerythrin-labeled streptavidin (Invitrogen) in PBST was added and incubated for 20 min. Finally, beads were washed and measured in 60 μl of PBST using a dedicated instrument (FlexMap3D, Luminex Corp.).

### 2.5. *Assessment of apparent detection limits*

Limits of detection were determined for both sample and antigen dilutions. For the sample dilution series, a pool of plasma samples was diluted over several concentrations in 1× PBS and then subjected to the 50× dilution in the assay buffer. For the detection limit assessment with antigen, a plasma pool was diluted 1:10 with 1× PBS, spiked with 0–50,000 ng/ml of recombinant CNDP1 (Origene) and diluted 50× in assay buffer, yielding a spike-in sample series with 0–1000 ng/ml CNDP1. All samples were heat treated before 45 μl were combined with 5 μl of the bead array, as described above. The apparent limit of detection was calculated using a five-parametric logistic regression as the concentration of spiked antigen corresponding to MFI values 3× standard deviation above background. A spike-in without replicates was included in the final assay of the phase IV sample collection, and detection limits were determined as 30% above the background intensity. For analysis with A2M (DY1938, RnD Systems), a spike-in series with 0–100 ng/ml antigen was prepared.

## 3. Data analysis

For each bead identity, 32 counted events were required as absolute minimum to qualify the median fluorescence intensity (MFI) for further analysis (personal communication with Luminex Corp.). All data processing and analysis was conducted using the R environment [15]. During phases III and IV the MFI values were corrected for order in the sequential readout; within each 96-well-assay plate using Pareto scaling (phase III) denoted scaled intensity and within each 384-well-assay plate using LOESS (phase IV) denoted nMFI, and used in further statistical analysis. The variability within a measurement was evaluated with the coefficient of variation (CV) as the ratio of standard deviation and mean and protein profiles both within and between measurements were correlated using Pearson's correlation test. The CV calculation was performed with nMFI adjusted so that the minimum intensity value per antibody equaled zero.

The association of the cancer associated confounder age and also total PSA plasma concentration was tested with a generalized linear model (GLM). The association between CNDP1 level and tumor stage was tested with a GLM including age as a covariate with data from sample sets in phases II–IV. For phase IV samples, the tumor stages were converted to integers from 1 to 3 for T0/T1, T2 and T3/T4, respectively. Furthermore Kruskal–Wallis one-way analysis of variance (KW) was used to assess the association between phase I's PCa risk

groups or phase IV's N or M stage sample groups and CNDP1 detection level. A GLM was applied to test for T stage associated protein profiles and Kruskal–Wallis rank sum test to determine N and M stage associated protein profiles. Multiple testing was accounted for using the Benjamini and Hochberg method.

The receiver operating characteristic (ROC) area under the curve (AUC) and 95% confidence interval (CI) with 2000 bootstrap replicates were calculated per antibody (phases I–III) and for all antibodies combined (phase IV) including available clinical covariates age, total PSA and the number of positive biopsies; in the classification between controls and advanced cases (phase I; low and high PCa risk, phase II and 3; indolent and aggressive PCa and phase IV; T0/T1 and T3/T4, N0 vs N1 and M0 vs M1 sample groups). The multivariate models were fitted using a generalized linear model (R-package GLM) prior ROC analysis (R-package pROC).

### 3.1. *Mass spectrometric analysis of immunocapture*

EDTA plasma was provided by Atlas Antibodies AB, Sweden and originated from three males and three females all without known disease diagnosis. This mixture of plasma was diluted 1:300 in assay buffer and heat treated as above. Antibodies HPA-1, MAB-1.1 and normal rabbit IgG (CAB-5) and normal mouse IgG (sc-2025, Santa Cruz Biotechnology) were coupled to Luminex beads as above, and beads carrying the different antibodies were incubated separately with 1 ml of heat treated plasma samples overnight at RT on gentle rotation. After incubation beads were washed 3× in PBS/0.03% CHAPS (Sigma) and 2× in 0.03% CHAPS, to be then re-suspended in 50 μl ammonium bicarbonate 50 mM to perform on beads trypsin digestion. Captured proteins were reduced with dithiothreitol (DTT) 1 mM and alkylated by iodoacetamide (IAA) 4 mM. Alkylation was quenched adding 1 mM DTT. Proteins were digested by trypsin (Promega) overnight at 37 °C and peptides were separated from beads, dried and re-suspended in buffer A (97% water, 3% acetonitrile (ACN), 0.1% formic acid (FA)).

In each LC–MS run, the LC auto sampler (HPLC 1200 system, Agilent Technologies) injected 5 μl of sample into a C18 guard desalting column (Zorbax 300SB-C18, 5 mm × 0.3 mm, 5 μm bead size, Agilent). We then used a 15 cm long C18 picofrit column (100 μm internal diameter, 5 μm bead size, Nikkyo Technos Co., Tokyo, Japan) installed on to the nano electrospray ionization (NSI) source. Solvent A was 97% water, 3% acetonitrile (ACN), 0.1% formic acid (FA); and solvent B was 5% water, 95% ACN, 0.1% FA. At a constant flow of 0.4 μl/min, the linear gradient went from 2% B up to 40% B in 45 min, followed by a steep increase to 100% B in 5 min. Online LC–MS was performed using a hybrid LTQ-Orbitrap Velos mass spectrometer (Thermo Scientific). Precursors were isolated with a 2 *m/z* window. We enabled "preview mode" for FTMS master scans, which proceeded at resolution of 30,000 (profile mode). Data-dependent MS/MS (centroid mode) followed in two stages: firstly, the top 5 ions from the master scan were selected for collision induced dissociation (CID, at 35% energy) with detection in the ion trap (ITMS); and after, the same 5 ions underwent higher energy collision dissociation (HCD, at 37.5% energy) with detection in the orbitrap (FTMS).

All MS/MS spectra were searched by Sequest under the software platform Proteome Discoverer (PD, v1.3.0.339, Thermo Scientific) using a target-decoy strategy. The reference database used was the human reference proteome set from uniprot.org (2013-04-18). Precursor mass tolerance of 10 ppm and product mass tolerances of 0.02 Da for HCD-FTMS and 0.36 Da for CID-ITMS were used. Additional settings were: trypsin with 1 missed cleavage; carbamidomethylation on cysteine as fixed modification; and oxidation of methionine as variable modification. Precursor peak areas were quantified using the "precursor ions area detector" module of Proteome Discoverer. Peptides found at 1% FDR (false discovery rate) were used by the protein grouping algorithm in PD to infer protein identities.

## 4. Results

In the presented study, we investigated CNDP1 glycosylation in plasma by using Western blot analysis and developed sandwich immunoassays by raising monoclonal anti-CNDP1 antibodies. These binders were then epitope mapped for identifying matching pairs of antibodies to develop sandwich assays. During four rounds of analysis, here called phases I–IV, these assays were utilized to determine difference in CNDP1 plasma levels through in sample sets from two independent cohorts, as outlined in Fig. 1.

### 4.1. *Analysis of CNDP1 glycosylation*

In previous work [5], Western blot analysis of plasma revealed bands at ±55 kDa and ±150 kDa when using HPA008933 (denoted HPA-1). To investigate whether glycosylation of plasma CNDP1 plays a role in the differential profiles of aggressive and less aggressive forms, plasma as well as recombinant CNDP1 protein were exposed to PNGaseF treatment to facilitate enzymatic removal of predicted N-linked glycan structures. As shown in Fig. 2A for recombinant CNDP1, two proximate bands were observed at ±55 kDa and upon incubation with PNGaseF the upper band disappeared, which suggested that one CNDP1 isoform was glycosylated when expressed in HEK293T cells alongside an isoform that appeared not to carry a glycosylation. In plasma, PNGaseF treatment of controls and cases (group at risk) was effective for both to a similar extend and a shift toward lower molecular masses was observed for bands at ±55 kDa as well as the band at ±150 kDa (Fig. 2B and C). Importantly, the bands at now ±50 kDa revealed concordant decrease in intensity as found in previous observations and analysis of plasma without PNGaseF. This suggests that glycosylation status of CNDP1 detected in Western blot analysis did not differ between case and control groups.

### 4.2. *Generation and characterization of CNDP1 antibodies*

A main aim of this study was to develop sandwich immunoassays for CNDP1 to determine the protein in plasma other then using discovery tools such as antibody arrays and to allow for a better selectivity of the analysis. For this matter, monoclonal

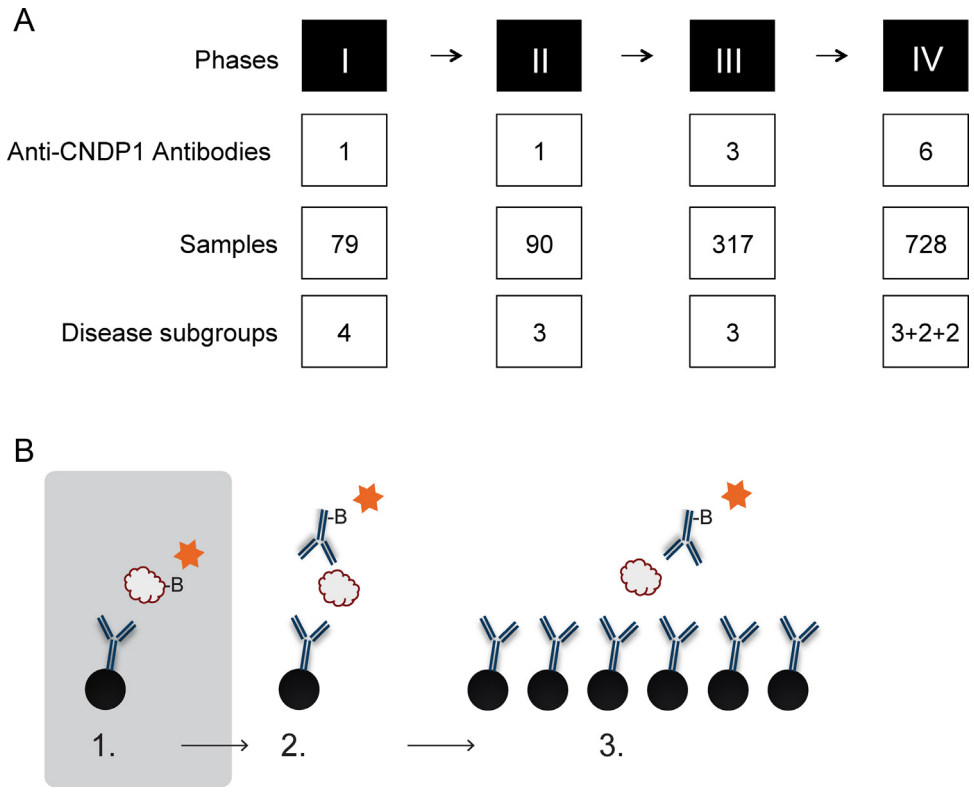


**Fig. 1 – Study overview. (A) The investigation of CNDP1 in relation to prostate cancer was organized into phases I–IV using particular plasma sample collections for each. (B) The illustration refers to the transition of single binder discovery to analysis with bead based sandwich immunoassays that used several different capture antibodies targeting CNDP1 in parallel.**

antibodies toward residues 32–133 of CNDP1 were raised. Prior to further analysis, all antibodies listed (Supplementary Table 1) were epitope mapped using peptide bead arrays of 15-mer peptides covering two CNDP1 fragments covering N-terminal residues, respectively (Fig. 3A). As previously described [14], this information was then further used to purify fractions form the polyclonal antibody HPA-1 based on peptides. Out of a total of 23 antibodies, including HPAs, MABs and CABs, CNDP1 epitope maps of 6 were shown in Fig. 3.

In addition, Western blot analysis was performed using plasma, and as shown in Supplementary Figure 1, congruent, single bands between 50 and 75 kDa were observed for the two monoclonal antibodies (MAB-1.1 and MAB-1.2) as well as HPA-1 and HPA-1.F15. As a note, antibodies raised against CNDP2 did not reveal any bands in the MW range of CNDP1. A second band observed at ±150 kDa was common for HPA-1, HPA-1.F15 as well as for CAB-1. Upon comparing this to the detection using an antibody toward alpha-2-macroglublin (A2M; HPA002265 listed as HPA-5), a plasma protein known to interact with proteases [11], a band at 150 kDa was most prominent besides other at higher and lower molecular masses (Supplementary Figure 1). This observation either suggests that the complex CNDP1 and A2M interacting via A2M's bait region was detected in plasma when assuming that two different antibodies (HPA-1, HPA-1.F15 and CAB-1) used for Western blot analysis reveal a specific detection of CNDP1. Otherwise, it suggested that the two antibodies also recognize an isoform of A2M of about 150 kDa in Western blot analysis. To further study this observation, sandwich assays for CNDP1 (see below) and A2M were used in parallel by applying each of these respective detection antibodies separately onto one bead array built with CNDP1 and A2M antibodies. As shown in Supplementary Figure 2 using spiked recombinant CNDP1 or A2M, no substantial degree of off-target recognition was observed and therefore suggested that A2M was not recognized by the employed CNDP1 sandwich assays.

We further utilized mass spectrometry to identify proteins being captured by antibodies immobilized on beads. As summarized in Fig. 3B for HPA-1 and MAB-1.1 several CNDP1 peptides were identified as being captured and being discrete from analysis performed using either normal rabbit IgG (CAB-5) or normal mouse IgG. This again supported that previous single antibody capture analysis [5] revealed profiles of CNDP1 and also did not revealed any presence of A2M.

### 4.3. *Development of sandwich immunoassays*

To select antibodies for the detection of CNDP1 via a sandwich immunoassay, all antibodies were coupled to distinct bead populations for a parallel capture reaction. Each capture antibody targeted mapped regions of CNDP1 (Supplementary Table 1) and different detection antibodies were evaluated for to build matching pairs. Using plasma samples to assess the performance, 3× HPA, 1× CAB and 2× MAB antibodies

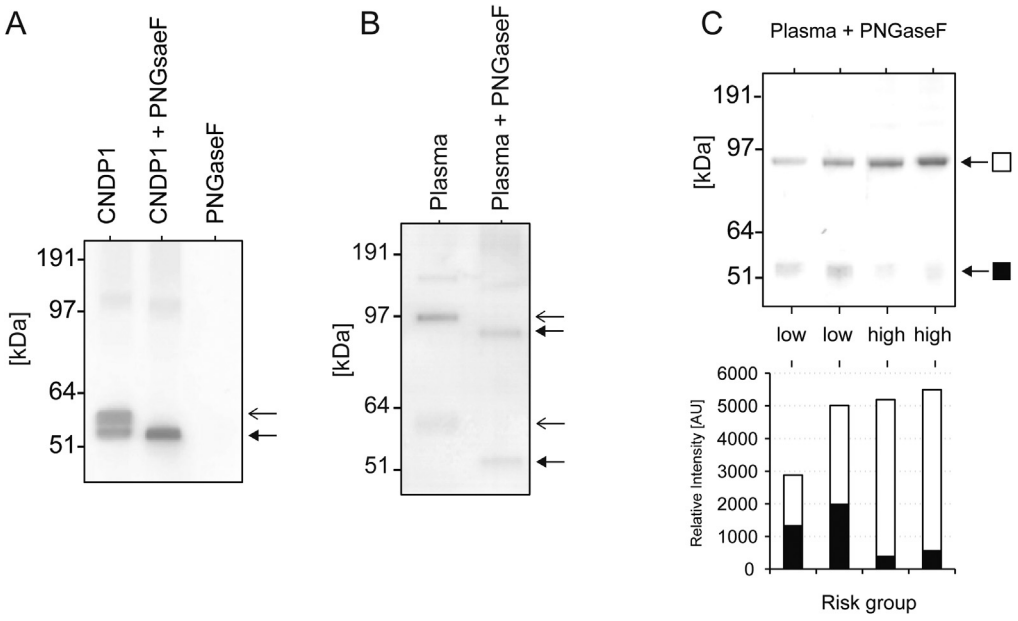


**Fig. 2 – Western blot analysis of CNDP1 N-glycosylation. (A) Recombinant CNDP1, (B) a plasma pool and (C) 4 individual plasma samples from the phase I sample collection with high and low PCa risk, exposed to PNGaseF (+). (A) The apparent molecular mass of the recombinant protein CNDP1 decreased with exposure to PNGaseF (indicated with arrows) and no upper band was detected. (B, C) Both the upper and lower bands (indicated with arrows) shifted in apparent molecular mass with exposure to PNGaseF. (C) Relative WB intensity of protein bands between 51 and 64 kDa (lower band) comparing samples from individuals with low and high risk for prostate cancer were concordant with results from the sandwich immunoassay (data not shown here). PNGaseF referred to Peptide-N-glycosidase F and (+) indicated that samples were exposed to this enzyme.**

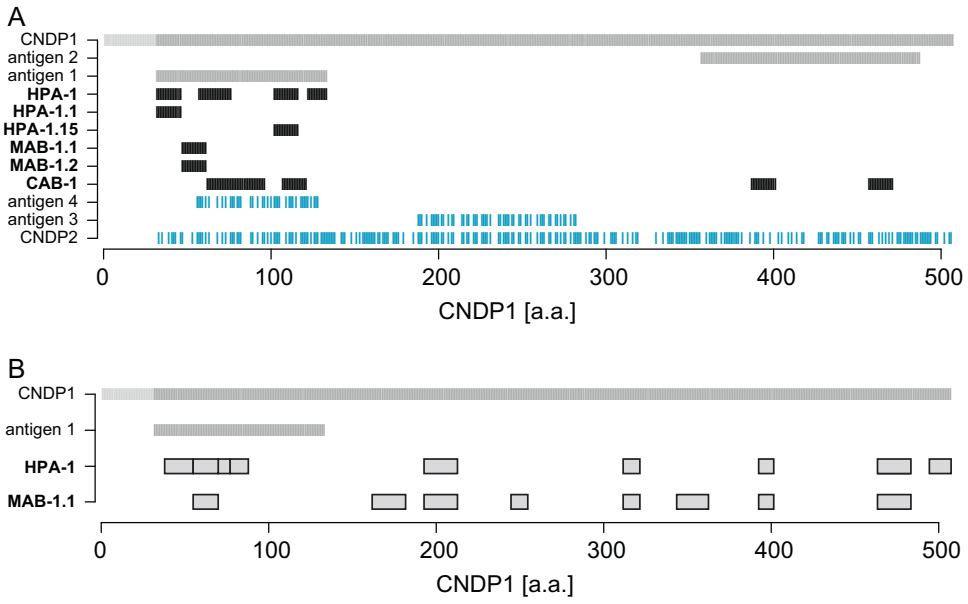


**Fig. 3 – CNDP1 epitopes and peptides. (A) Protein sequences of CNDP1 (gray bar, top) and CNDP2 (blue bar, bottom) were aligned to display antigens, epitope regions for the antibodies HPA-1, 1.1 and 1.15, MAB-1.1 and 1.2 and CAB-1 (black bar). (B) Mass spectrometric analysis of immunoprecipitated proteins captured from plasma using beads coupled with HPA-1 or MAB-1.1 revealed several CNDP1 peptides. (For interpretation of the references to color in this figure legend, the reader is referred to the web version of this article.)**

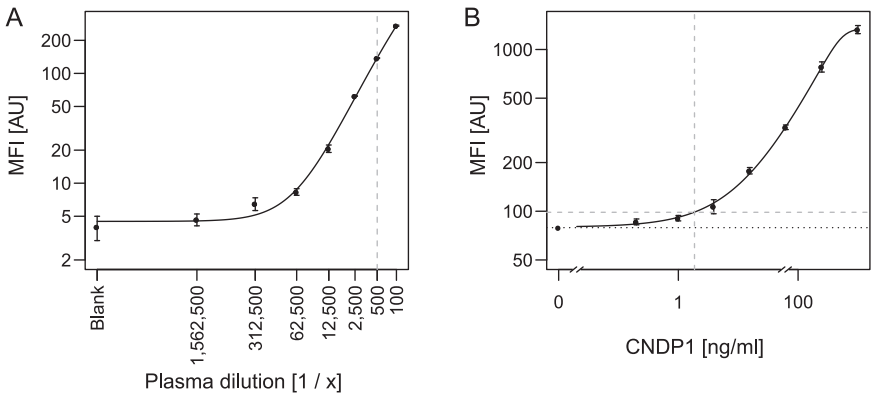


**Fig. 4 – Sandwich assay for CNDP1. (A) Plasma was diluted in a series of concentrations and analyzed with sandwich pair of HPA-1 and CAB-1 and a sample dilution factor of 1/500 (gray dashed line) was used for the subsequent sandwich immunoassays. (B) The apparent limit of detection was determined at 2 ng/ml using recombinant protein CNDP1 spiked into diluted plasma. Vertical dashed line: detection limit; horizontal dashed line: 3× standard deviation above background; Dotted line: background.**

chosen as capture reagent revealed the highest intensity fold change, when comparing samples with low and high PCa risk. In addition, apparent limit of detection (<30 ng/ml) and technical variance (CV < 10%) were used as selection criteria for employing 6 different antibodies in further analysis, as shown in Table 1 and in combination with a polyclonal detection antibody (CAB-1). A sample dilution series was analyzed with two sandwich immunoassays (Fig. 4 and Supplementary figure 3) and intensities from CNDP1 targeting pairs decreased with sample dilution, following a sigmoidal dilution curve. For the following analysis of patient samples (phase IV), we supplemented the 6 capture antibodies with 4 other antibodies and one empty bead (Table 1) to confirm the detected levels of CNDP1 in association to PCa severity via different epitopes.

### 4.4. *Analysis of CNDP1 in two prostate cancer patient cohorts*

At first, previous results generated with the single binder assay from the analysis of the discovery cohort (phase I, $n = 79$) and first verification (phase II, $n = 90$) sample sets [5] were reproduced with the sandwich assays using the pair HPA-1 with CAB-1 (Fig. 5A and B). For phases I/II, the data showed a separation of $p = 0.0004$ (KW, CNDP1 ~ PCa risk) and $p = 0.006$ (GLM, CNDP1 ~ PCa stage) and ROC AUCs 0.84 and 0.67 (Table 2; Supplementary Figure 4). There was no statistically significant association between age-adjusted CNDP1 intensity and PCa stage (GLM $p > 0.05$, age-adjusted-CNDP1 ~ PCa stage). Next, the analysis was extended into phase III sample collection ($n = 368$; Fig. 5C). There, no statistically significant association of CNDP1 with aggressive prostate cancer was found (GLM $p > 0.05$) nor did CNDP1 outperform total PSA or age in ROC analysis, as shown in Table 2.

We continued with analyzing a new sample collection, denoted phase IV, that was built on 728 samples. In this analysis, the detected levels of CNDP1 highly correlated between the 6 antibodies (rho 0.84–0.97), and a decrease in CNDP1 was found for primary tumor stage T3 and T4, distant metastasis M1 and in samples annotated with PCa spreading to regional lymph nodes N1 (Fig. 6). When combining the data from all CNDP1 antibodies into one classifier, an improved separation in the comparisons of M1 vs M0, N1 vs N0 or T3/T4 vs T0/T1

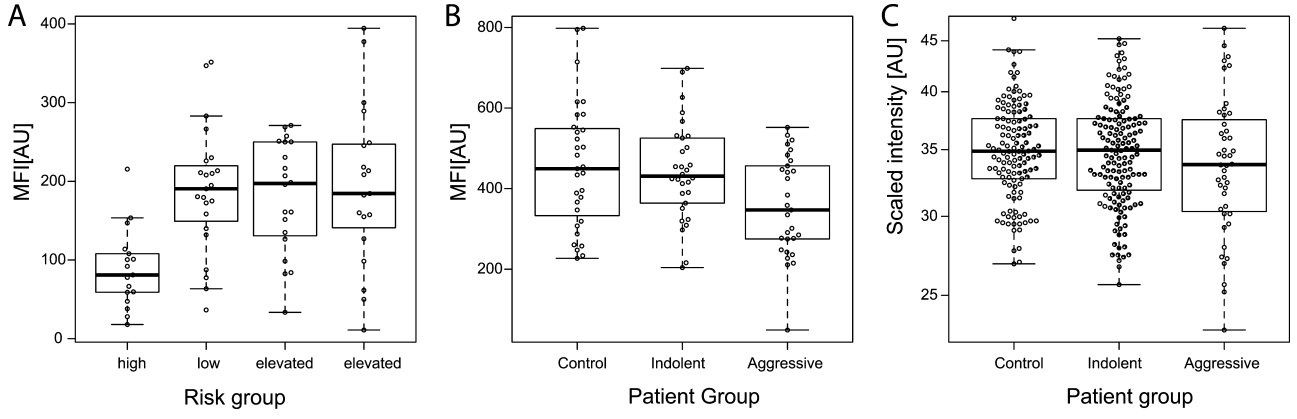


**Fig. 5 – CNDP1 sandwich assays. The boxplots display CNDP1 intensity ranges per sample group for the sample collections (A) phase I, (B) phase II, and (C) phase III using capture antibody HPA-1 and CAB-1 for detection.**

**Table 2 – Classification of PCa risk or aggressive PCa with ROC analysis. The variables CNDP1 intensity, total plasma PSA and age (age available for phases II and III) were included in the classification analysis, multivariate models fitted using a GLM and the performance of each classification evaluated via AUC values with 95% confidence intervals.**

| Phase | Antibody | Comparison (samples) | Variables | AUC | CI |
|---|---|---|---|---|---|
| I | [a] | High ($n=17$) vs Low risk ($n=23$) | tPSA | 1.00 | 1.0–1.0 |
| | HPA-1 | | CNDP1 + tPSA | 1.00 | 1.0–1.0 |
| | HPA-1 | | CNDP1 | 0.84 | 0.7–1.0 |
| II | HPA-1 | Indolent ($n=30$) vs Aggressive ($n=29$) | tPSA/age + tPSA/CNDP1 + age + tPSA | 1.00 | 1.0–1.0 |
| | HPA-1 | | CNDP1 + age | 0.91 | 0.8–1.0 |
| | [a] | | Age | 0.81 | 0.7–0.9 |
| | HPA-1 | | CNDP1 | 0.67 | 0.5–0.8 |
| III | HPA-1[b] | Indolent ($n=147$) vs Aggressive ($n=44$) | Age + tPSA/age + CNDP1 + tPSA | 0.90 | 0.9–1.0 |
| | HPA-1[b] | | Age + CNDP1/Age | 0.85 | 0.8–0.9 |
| | [a] | | tPSA | 0.73 | 0.6–0.8 |
| | HPA-1.F15 | | CNDP1 | 0.56 | 0.5–0.7 |
| | HPA-1.F1 | | CNDP1 | 0.55 | 0.4–0.7 |
| | HPA-1 | | CNDP1 | 0.55 | 0.5–0.6 |

[a] Clinical data only.
[b] As well as HPA-1.F1 or HPA-1.F15.

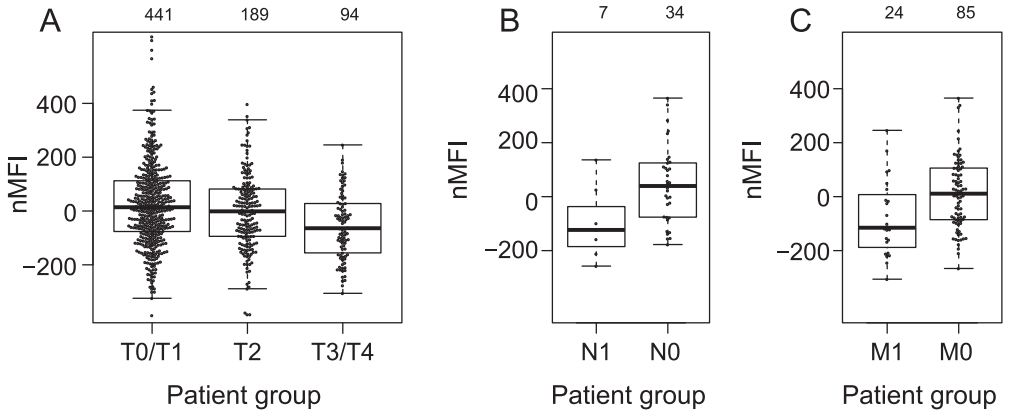


**Fig. 6 – CNDP1 levels in tumors. The level of CNDP1 detected in samples from phase IV using a sandwich assay. Lower detection levels (nMFI) of CNDP1 were observed with all 6 antibody pairs in sample subsets corresponding to the most advanced stages of PCa; (A) T3/T4, (B) N1 and (C) M1, here displayed with data from a sandwich assay with a monoclonal capture (MAB-1.1) and polyclonal detection (CAB-1) antibody anti-CNDP1. The numbers of samples within each sample group were listed in the figure.**

was achieved (Table 3A–C, Supplementary Table 2B). CNDP1 intensity profiles classified tumor stages T0/T1 from T3/T4 with AUC 0.77 when combing all pairs and age, but again total PSA levels outperformed even a classification including CNDP1, age, gender and the number of positive biopsies (Table 3A). CNDP1 showed to improve the classification for total PSA in the comparison of M1 vs M0 stages when combined with age (AUC = 0.95, Table 3B). Most interestingly, when using CNDP1 and age in the classification of N1 vs N0 samples, plasma CNDP1 levels resulted in an improved classification compared to total PSA, age or the number of positive biopsies (AUC ranged 0.66–0.87, Table 3C). In essence, CNDP1 did not outperform total PSA when comparing prostate cancer patient M or T stages, but it showed to improve the detection of regional lymph node metastasis when differentiating between N1 and N0.

## 5. Discussion

In the presented study, plasma from more than 1000 individuals was analyzed in the context of prostate cancer using a sandwich immunoassay developed for the protein CNDP1. Our study included epitope mapping of antibodies, the development of a multiplexed, single-target sandwich immunoassay and investigations to resolve protein glycosylation. We confirmed decreasing CNDP1 levels in plasma of patients at a later stage of prostate cancer, in particular of those classified with metastasis of the lymph nodes.

Today, PSA is the only biomarker used in daily practice for diagnosis and in follow-up of prostate cancer patients. Although recent improvements in imaging by multimodality MRI and PET/CT scan, we lack a sensitive method to detect

**Table 3 – Classification of tumor stage with ROC analysis. The variables CNDP1 intensity, total plasma PSA, age and the number of positive biopsies were included in the classification analysis of (A) primary tumor stage (T0/T1 vs T3/T4), (B) distant metastasis (M0 vs M1) and (C) presence of metastasis in regional lymph nodes (N0 vs N1). Multivariate models were fitted using a GLM and the performance of each classification was evaluated via AUC values with 95% confidence intervals (CI).**

(A) T stages

| Capture antibody | Variable | AUC | CI |
|---|---|---|---|
| [b] | tPSA | 0.88 | 0.8–0.9 |
| Antibody panel[a] | CNDP1 + age + biopsy + tPSA | 0.87 | 0.8–0.9 |
| Antibody panel[a] | CNDP1 + age + tPSA | 0.86 | 0.8–0.9 |
| [b] | Age + tPSA | 0.85 | 0.8–0.9 |
| Antibody panel[a] | CNDP1 + age + biopsy | 0.78 | 0.7–0.8 |
| Antibody panel[a] | CNDP1 + age | 0.77 | 0.7–0.8 |
| MAB-1.1; MAB-1.2 or HPA-1.F15 | CNDP1 + age | 0.76 | 0.7–0.8 |
| CAB 1; HPA-1 or HPA-1.F1 | CNDP1 + age | 0.75 | 0.7–0.8 |
| [b] | Age | 0.74 | 0.7–0.8 |
| [b] | Biopsy | 0.67 | 0.6–0.7 |

(B) M stages

| Antibody | Variable | AUC | CI |
|---|---|---|---|
| Antibody panel[a] | CNDP1 + age + tPSA | 0.95 | 0.9–1.0 |
| Antibody panel[a] | CNDP1 + age + biopsy + tPSA | 0.94 | 0.9–1.0 |
| [b] | Age + tPSA | 0.93 | 0.9–1.0 |
| [b] | tPSA | 0.92 | 0.8–1.0 |
| Antibody panel[a] | CNDP1 + age + biopsy | 0.75 | 0.6–0.9 |
| Antibody panel[a] | CNDP1 + age | 0.73 | 0.6–0.9 |
| HPA-1.F1 | CNDP1 + age | 0.71 | 0.6–0.8 |
| MAB-1.1 | CNDP1 + age | 0.70 | 0.6–0.8 |
| MAB-1.2 | CNDP1 + age | 0.68 | 0.6–0.8 |
| HPA-1 or HPA-1.F15 | CNDP1 + age | 0.67 | 0.5–0.8 |
| CAB-1 | CNDP1 + age | 0.64 | 0.5–0.8 |
| [b] | Biopsy | 0.62 | 0.5–0.7 |
| [b] | Age | 0.54 | 0.4–0.7 |

(C) N stages

| Capture antibody | Variable | AUC | CI |
|---|---|---|---|
| Antibody panel[a] | CNDP1 + age + biopsy + tPSA | 0.94 | 0.9–1.0 |
| Antibody panel[a] | CNDP1 + age + biopsy | 0.91 | 0.8–1.0 |
| Antibody panel[a] | CNDP1 + age + tPSA | 0.90 | 0.8–1.0 |
| Antibody panel[a] | CNDP1 + age | 0.87 | 0.7–1.0 |
| HPA-1.F1 | CNDP1 + age | 0.76 | 0.5–1.0 |
| MAB-1.2 | CNDP1 + age | 0.75 | 0.5–1.0 |
| MAB-1.1 | CNDP1 + age | 0.74 | 0.5–1.0 |
| HPA-1 or HPA-1.F15 | CNDP1 + age | 0.70 | 0.4–1.0 |
| CAB 1 | CNDP1 + age | 0.66 | 0.4–1.0 |
| [b] | Age + tPSA | 0.62 | 0.4–0.9 |
| [b] | Biopsy | 0.62 | 0.4–0.9 |
| [b] | Age | 0.61 | 0.4–0.9 |
| [b] | tPSA | 0.58 | 0.3–0.9 |

[a] Antibody panel: HPA-1; HPA-1.1; HPA-1.15; MAB-1.1; MAB-1.2 and CAB-1.
[b] Clinical data only.

lymph node metastases in prostate cancer patients. Surgical lymph node dissection is still golden standard thus new markers to predict increase risk of lymph node metastases are highly warranted. Our study therefore suggests investigating CNDP1 further using functional analysis to elucidate, which mechanisms contribute to its decreasing plasma levels and how such changes can be addressed by therapy. Hereby, a focus could be on lymphatic systems and its contribution to decreases of CNDP1, but it will also be required to assess whether this is a prostate or gender specific finding. There were a few number of N1 cases in the analyzed cohorts, so further replication in independent sample collections and cohorts is anticipated to confirm the observed relation of CNDP1 to advanced PCa.

We had previously speculated on the influence of glycosylation status on CNDP1 detection [5]. It is known that carbohydrate components of glycoproteins perform critical biological functions in protein sorting, immune and receptor recognition, inflammation, pathogenicity, metastasis, and other cellular processes [16]. N-glycans may play a role in

cancer progression, as malignant cells have been shown to synthesize longer chains of N-glycans [17,18] and alterations of specific glycans have been observed in metastatic prostate cancer [19]. Using antibody-based detection in combination with plasma and recombinant protein being subjected to enzymatic deglycosylation, we could not find that indications of CNDP1 level decrease were primarily effected by their state of glycosylation. Further analysis would be required to better understand CNDP1 glycosylation in prostate cancer, but our current data did not support previous speculations, as differential detection of CNDP1 appeared unrelated to glycosylation.

Also, the relation of detected protein levels where corroborated for off-target detection. First for CNDP2, a peptidase found as a cytosolic homodimer with 2 acetylation sites and has recently been found in proteomic analysis of Parkinson's disease [20]. CNDP2 has a 55% sequence similarity to CNDP1 but as shown by the panel of applied capture antibodies, our data did not reveal that CNDP2 would be detected instead of CNDP1. The highly abundant protease inhibitor A2M, which can form a stable complex with CNDP1, was hypothesized to constitute the approximately 150 kDa protein band observed with WB using HPA-1, HPA-1.F15 and CAB-1, as A2M or A2M-CNDP1. The interaction between A2M and anti-CNDP1 HPA-1, CAB-1, MAB-1.1 and MAB-1.2 were studied using sandwich assays. There, no cross-reactivity toward A2M protein was observed thus suggesting that the second band in Western blot analysis was either not A2M or particular to the Western blot analysis. Given that Western blot display proteins enriched at their respective molecular mass location, the higher local density of A2M regions similar to CNDP1 may have lead this antibody to recognize A2M. We also demonstrate the possibility to combine mass spectrometric read-out with bead based assays, as proteins being captured by the immobilized antibodies can be identified as being CNDP1 specific by on bead trypsin digestion. Even though this was achieved on a single sample only, it supports this and previous studies in providing evidence for CNDP1 detection in plasma. In the mass spectrometric analysis, no peptides were assigned to A2M and strengthen the above observation of an A2M-free isoform of CNDP1.

To our current knowledge, this is one of the first studies that follows up on discoveries made with antibody arrays and it also represents a path on how to develop sandwich assays from such single binder assays. This may therefore be an important and noteworthy contribution to existing proteomic studies in plasma, as it addresses the challenge of off-target binding through the use of several antibodies with distinct epitopes on one target protein. Further so, we anticipate that proteins detectable in plasma with single binder assays, such as PSA [5], should also be detectable using sandwich assays. Nevertheless, sandwich assays are still not a fist line tool to discover new candidates for disease classification, thus argue for new sandwich assay technologies to be developed for a first line discovery. Until then, single binder assays may remain a first choice in affinity proteomics during screening, but preferably not during verification. Multiplexing offers the inclusion of several target assays into a single analysis. Rather than supplementing other target assays, we chose to determine one protein via parallel capture reactions through the detection with one detection antibody. It might be argued for that using a single detection antibody could still not rule out that off-target interactions are being measured. But as shown here by the use of six capture antibodies that were generated in different species, targeting different epitopes, while being utilized in a multiplex fashion, correlating intensity profiles (median rho 0.93) were obtained to support the detection of CNDP1.

In conclusion, our study shows the development and application of a multiplexed sandwich assay for a single target via the use of distinct epitopes of CNDP1. This confirmed decreasing levels of CNDP1 in plasma from patients suffering from prostate cancer and revealed that CNDP1 levels were particularly different in patients with diagnosed lymph node metastasis. This refined understanding of CNDP1 association may contribute to alternative detection of prostate cancer and lymph node status.

## Acknowledgements

We like to thank the entire staff of the Human Protein Atlas for their efforts. From Karolinska Institute, we thank Martin Eklund for statistical support and Janne Lehtiö for fruitful discussions. This study was funded by grants from Science for Life Laboratory Stockholm, by the ProNova VINN Excellence Centre for Protein Technology (VINNOVA, Swedish Governmental Agency for Innovation Systems), by grants from the Knut and Alice Wallenberg Foundation and the European Union 6th Framework P-Mark (Grant number LSHC-CT-2004-503011), Swedish Cancer Society, and Swedish Research Council Medicine (VR).

## Appendix A. Supplementary data

Supplementary data associated with this article can be found, in the online version, at doi:10.1016/j.trprot.2013.12.001.

## REFERENCES

[1] Pin E, Fredolini C, Petricoin 3rd EF. The role of proteomics in prostate cancer research: biomarker discovery and validation. Clin Biochem 2013;46:524–38.
[2] Stoevesandt O, Taussig MJ. Affinity proteomics: the role of specific binding reagents in human proteome analysis. Expert Rev Proteomics 2012;9:401–14.
[3] Ayoglu B, Haggmark A, Neiman M, Igel U, Uhlen M, Schwenk JM, et al. Systematic antibody and antigen-based proteomic profiling with microarrays. Expert Rev Mol Diagn 2011;11:219–34.
[4] Fagerberg L, Oksvold P, Skogs M, Algenas C, Lundberg E, Ponten F, et al. Contribution of antibody-based protein profiling to the human chromosome-centric proteome project (C-HPP). J Proteome Res 2013;12(6):2439–48.
[5] Schwenk JM, Igel U, Neiman M, Langen H, Becker C, Bjartell A, et al. Toward next generation plasma profiling via heat-induced epitope retrieval and array-based assays. Mol Cell Proteomics 2010;9:2497–507.
[6] Peters V, Jansen EE, Jakobs C, Riedl E, Janssen B, Yard BA, et al. Anserine inhibits carnosine degradation but in human serum carnosinase (CN1) is not correlated with histidine dipeptide concentration. Clin Chim Acta 2011;412:263–7.

[7] Adelmann K, Frey D, Riedl E, Koeppel H, Pfister F, Peters V, et al. Different conformational forms of serum carnosinase detected by a newly developed sandwich ELISA for the measurements of carnosinase concentrations. Amino Acids 2012;43:143–51.
[8] Lenney JF, George RP, Weiss AM, Kucera CM, Chan PW, Rinzler GS. Human serum carnosinase: characterization, distinction from cellular carnosinase, and activation by cadmium. Clin Chim Acta/Int J Clin Chem 1982;123:221–31.
[9] Teufel M, Saudek V, Ledig JP, Bernhardt A, Boularand S, Carreau A, et al. Sequence identification and characterization of human carnosinase and a closely related non-specific dipeptidase. J Biol Chem 2003;278:6521–31.
[10] Liu T, Qian WJ, Gritsenko MA, Camp 2nd DG, Monroe ME, Moore RJ, et al. Human plasma N-glycoproteome analysis by immunoaffinity subtraction, hydrazide chemistry, and mass spectrometry. J Proteome Res 2005;4:2070–80.
[11] Burgess EF, Ham AJ, Tabb DL, Billheimer D, Roth BJ, Chang SS, et al. Prostate cancer serum biomarker discovery through proteomic analysis of alpha-2 macroglobulin protein complexes. Proteomics Clin Appl 2008;2:1223.
[12] Ahluwalia TS, Lindholm E, Groop LC. Common variants in CNDP1 and CNDP2, and risk of nephropathy in type 2 diabetes. Diabetologia 2011;54:2295–302.
[13] Janssen B, Hohenadel D, Brinkkoetter P, Peters V, Rind N, Fischer C, et al. Carnosine as a protective factor in diabetic nephropathy: association with a leucine repeat of the carnosinase gene CNDP1. Diabetes 2005;54:2320–7.
[14] Hjelm B, Forsstrom B, Igel U, Johannesson H, Stadler C, Lundberg E, et al. Generation of monospecific antibodies based on affinity capture of polyclonal antibodies. Protein Sci 2011;20:1824–35.
[15] R Development Core Team. R: a language and environment for statistical computing. Vienna, Austria: R Foundation for Statistical Computing; 2011.
[16] Magnelli P, Bielik A, Guthrie E. Identification and characterization of protein glycosylation using specific endo- and exoglycosidases. Methods Mol Biol 2012;801:189–211.
[17] Buck CA, Glick MC, Warren L. Glycopeptides from the surface of control and virus-transformed cells. Science 1971;172:169–71.
[18] Kyselova Z, Mechref Y, Al Bataineh MM, Dobrolecki LE, Hickey RJ, Vinson J, et al. Alterations in the serum glycome due to metastatic prostate cancer. J Proteome Res 2007;6:1822–32.
[19] Lau KS, Dennis JW. N-glycans in cancer progression. Glycobiology 2008;18:750–60.
[20] Licker V, Cote M, Lobrinus JA, Rodrigo N, Kovari E, Hochstrasser DF, et al. Proteomic profiling of the substantia nigra demonstrates CNDP2 overexpression in Parkinson's disease. J Proteomics 2012;75:4656–67.